

THE EFFECT OF NANOCALCITE-MODIFIED EPOXY RESINS ON THE MECHANICAL PROPERTIES AND TENSILE FATIGUE PERFORMANCE OF GLASS REINFORCED COMPOSITES

Douglas Goetz, James Nelson, Jay Lomeda, Wendy Thompson, Paul Sedgwick
3M Advanced Composites
3M Center, St. Paul, MN 55144

Rick Lowery, Jeff Okeke, Dustin Davis
Norplex-Micarta, Postville, IA 52162

ABSTRACT

The effect of nanocalcite-modified epoxy matrix resins on the mechanical properties and tensile fatigue performance of glass-reinforced composites was examined. Glass fabric reinforced composite laminates were created using an industry-standard epoxy matrix as a control material and 3M Matrix Resin 8835 (MR 8835), an epoxy resin having a high loading of surface-functionalized nanoscale calcite particles. Incorporation of a high loading of calcite nano-scale particles lead to improvements in composite compression strength and through-thickness properties. The tensile static and stress-controlled fatigue behavior of the MR 8835-based laminates were examined in both the resin-dominated $\pm 45^\circ$ and the fiber-dominated 0° directions. Static tensile modulus and strength were higher for the nanocalcite-modified laminates for both orientations. Stress-life curves, cyclic stress-strain loops, and reduction of stiffness during cycling data were obtained from fatigue testing. Fatigue performance in the $\pm 45^\circ$ orientation was dramatically improved for nanocalcite-modified laminates relative to the standard laminate. Fatigue life was improved up to 65 times over the control material and resistance to increasing mean strain (ratcheting) was much greater for the MR 8835-based composite. Additionally, retention of laminate stiffness was greatly improved. The 0° tensile fatigue performance was also dramatically improved, with fatigue life improvements of greater than 10 times the life of the control material. Laminate stiffness was greatly increased over the entire life for all stress levels tested. Peak strain levels were significantly lower than for the control material at comparable stress levels.

1. INTRODUCTION

The focus of this study is the effect of nanocalcite-modified epoxy resins on the mechanical properties and tensile fatigue performance of glass fabric-reinforced composites. A brief review of the characteristics of this type of nanoparticle-modified matrix resin composites follows, and the rationale and plan for the study are given.

1.1 Background: Inorganic Nanoparticle Modification of Matrix Resins

The incorporation of a high level of well-dispersed, inorganic, nanoscale particles into the matrix polymer of a fiber-reinforced composite significantly alters key properties of the matrix, and therefore impacts the matrix-dominated properties of the composite. In addition, in some

situations fiber-dominated strength, most notably compression strength, is improved because of the dependence of the micromechanics of failure on matrix properties.

Previous work has illustrated how surface-functionalized low aspect-ratio inorganic particles can be used to produce highly-loaded thermosetting matrix resins while preserving the viscosity needed for composites processing, including prepregging, pultrusion, and filament winding [e.g., 1-5]. A primary effect is a dramatic increase in matrix modulus, well above the achievable maximum for unoriented, unfilled polymers. This increase has a direct impact on the micromechanics governing strength and the off-axis (shear and transverse) lamina stiffnesses. Composite compression strength, flexural strength, and interlaminar shear strength have been shown to increase for carbon fiber reinforced composites. Appropriate surface functionalization of the particles can simultaneously lead to an increase in the matrix fracture resistance. Other beneficial effects of highly-filled matrix resins include reduced matrix shrinkage, exotherm, higher hardness, lower water pick-up, and lower thermal distortion.

These increases in composite properties have been shown to translate into increased performance in drive shafts, composite overwrapped pressure vessels, composite tooling, and pultruded parts [2-5].

1.2 Motivation and Plan of This Study

Most composite structures are subjected to cyclic loading. In some cases, fatigue behavior is an explicit design driver. Even when fatigue analysis is not performed in the design of a composite structure, adequate fatigue performance is typically verified by laboratory or use testing.

Two characteristics of the type of nanoparticle-modified matrix resins here considered suggest a possible favorable effect on composite fatigue behavior. First, the enhanced matrix modulus is expected to produce altered load sharing between fiber reinforcement and the matrix both at the laminate and micro scale. Second, the distribution of nanoscale particles uniformly in the matrix may lead to damage resistance and arrest mechanisms at a very small scale, consistent with the nature of diffuse damage typically seen in composite fatigue.

Fatigue of nanosilica-modified glass reinforced composites has been explored previously in several studies. Most of these have addressed relatively low loading of particles, focusing on the unique toughening behavior of these systems. Significant improvements in stress-life and damage accumulation behavior were demonstrated [e.g., 6, 7]. The effect of high loadings of low-aspect ratio nanoparticles has been less studied. Makeev et al. showed improved static and fatigue performance in interlaminar shear for both glass and carbon fiber prepregs using 20 and 40 weight % nanosilica [8]. Improvement in the number of pressure cycles to liner through-cracking for carbon fiber composite overwrapped pressure vessels has been demonstrated for nanocalcite-modified resins [5]. The direct composite material response during cycling was not determined.

In contrast to prior work, this study examines behavior of composites with made using highly-filled nanocalcite-modified matrix resins. Two aspects of fatigue behavior are addressed: stress-life behavior and damage accumulation quantified through changes in laminate stiffness during load cycling. First, neat resin properties and key static laminate properties for a nanocalcite-modified and unfilled control systems are reported. Next, the monotonic tensile behavior for both

materials is examined in detail for plain weave glass fabric laminates in a $\pm 45^\circ$ orientation. Stress-controlled tension-tension fatigue testing is performed to generate stress-life curves. The stiffness degradation during cycling is monitored to produce stiffness-cycle data for each test as well as stress-strain hysteresis loops. The $\pm 45^\circ$ orientation represents a highly matrix-dominated situation. The same test protocol is then applied to the materials in a 0° laminate orientation to examine the fiber-dominated situation.

2. EXPERIMENTATION

2.1 Materials and Processing

The nanocalcite-modified resin system used in this study is 3M Matrix Resin 8835, which is a bisphenol-A epoxy solution in acetone containing a high concentration of uniformly dispersed surface-functionalized nanoscale calcite particles. It has been optimized for solvent prepregging processes. When cured catalytically with dicy/urea the concentration of calcite is typically 48% by weight, which is about 30% by volume, with all solvent removed. The control matrix resin is an industry standard epoxy resin. To demonstrate salient property differences for the cured matrix resins, a dicy/urea cure was used to cast plaques of neat resin between glass plates treated with mold release coating. The starting material for these castings was unsolvated.

Composite laminates were produced using a high-throughput proprietary solvent prepregging process and curative by Norplex-Micarta of Pottsville, Iowa. The reinforcement was a plain weave E-glass fabric (ASTM style 7642) [9]. Compression molding was used to produce composite laminates nominally 3.2 mm thick. The laminates had a $0^\circ/90^\circ$ laminate orientation, with the warp direction of each layer in the 0° direction. The resulting control laminates were representative of industry standard NEMA G10 material. In the following discussion, the laminates will simply be referred to as control and MR 8835 for the industry standard and nanocalcite-modified materials, respectively.

2.2 Testing Procedures

2.2.1 Neat Resin and General Laminate Testing

Cast plates were machined to make specimens for neat resin tensile testing, fracture toughness testing, and dynamic mechanical analysis (DMA). The cured resin specimen preparation and testing methods used to obtain neat resin properties were based on American Society for Testing and Materials (ASTM) standards, as will be indicated in the results section. All testing was conducted under ambient laboratory conditions.

2.2.2 Static Tensile and Fatigue

Specimens were tabbed using G10 fiberglass tabs with a 10° taper. 3M AF 163-2 film adhesive was used to bond the tabs in a press using a cure cycle of 121°C for 90 minutes. The distance between tabs was 152 mm. Individual specimens nominally 25.4 mm wide were cut from the tabbed plate using a diamond blade saw to produce 11 specimens per set. Three of these were used for static tensile testing and 8 for fatigue testing. Before testing the edges of each specimen were lightly sanded to remove damage from cutting.

Static tensile testing was conducted according to ASTM D 3039. The static behavior informed the choice of loading levels for fatigue testing.

Fatigue tests were conducted using a servohydraulic load frame with hydraulic grips. Sinusoidal tension-tension loading in closed loop load-control was imposed, while monitoring specimen strain using an extensometer (gage length of 25.4 mm) as well as grip displacement. The stress ratio, R , is the ratio of the minimum stress to the maximum stress imposed. For all tests, $R = 0.1$. All testing was done at laboratory ambient conditions. During load cycling, hysteretic heating can occur. Specimen temperature was continuously monitored using a thermocouple adhesively attached to a specimen face. To limit the temperature rise due to heating, a fan was used to improve heat transfer from the specimens. The frequency of loading was also adjusted between 0.5 and 4 Hz, with lower frequency used for higher strain loading. Specimen temperatures were kept below 30 °C. Stress cycling was carried out until complete specimen failure.

3. RESULTS

3.1 Matrix Properties

Table 1 summarizes neat resin data for MR 8835 and a suitable control cured with a dicy/urea catalytic system. Note that the composite laminates were made using a different, proprietary curative and process; these properties show relative effects believed to be similar to the in-situ matrix properties of the laminates. The modification of the calcite nanoparticles did not alter the glass transition temperature. Of special importance to the fatigue discussion that follows, the resin tensile modulus of MR 8835 was 236 % of the control resin modulus. The fracture toughness was increased slightly.

Table 1. Resin Mechanical Property Data: MR 8835 vs. Control

Resin	Calcite (wt%)	Glass Transition, T_g (°C) (ASTM E1640)	Tensile Modulus (GPa) (ASTM D638)	Fracture Toughness (MPa√m) (ASTM D5045)	Critical Energy Release Rate (J/m ²)
Control	0	140	2.8	0.53	86
MR 8835	48	142	6.6	0.88	100

3.2 Composite Properties: Compression and Through-Thickness Properties

Table 2 summarizes key static composite properties (aside from tensile properties) that were affected by the enhanced matrix properties. Of special note, the in-plane compression modulus and strength were significantly higher for the MR 8835 laminate. The modulus increase reflects the increased load sharing of the matrix for the plain weave fabric reinforced laminates, and may be in part due to greater support of the wavy fibers. The increase in 0° compression strength is remarkable. In work with unidirectional glass fiber laminates with a nanosilica-modified epoxy matrix, Uddin and Sun [10] found that compression strength was significantly increased, even for a relatively modest weight fraction of 15% nanosilica in the matrix. The cause of this effect was identified as suppressed fiber microbuckling, and it was shown that “the elastic-plastic microbuckling model [could] be used to predict the enhancement in the composite compressive

strength based on the stress-strain curve of the modified matrix.” Compression strength with higher loading of nanosilica was also demonstrated for carbon fiber laminates [1], but the results of this study and Uddin and Sun suggest that matrix modification with stiff inorganic particles may be especially beneficial for glass fiber reinforced laminates.

Although they are not the focus of this study, through-thickness properties are matrix-dominated. The through-thickness compression modulus is increased due to increased matrix modulus, and strength is increased. Unlike the 0° compression strength, the failure mechanism is not dominated by fiber microbuckling. The through-thickness coefficient of thermal expansion (CTE) is reduced due to the reduced CTE of the matrix resin. This reduction has been shown to reduce thermally-driven distortion or residual stress in curved parts [2].

Table 2. Static Glass-Fabric Laminate Data for MR 8835 and Control Matrix Resins.

Property	ASTM Test Method	MR 8835	Control	% change
0° Compression Modulus (GPa)	D6641	31.6	20.3	56
0° Compression Strength (MPa)	D6641	434	332	31
Through-thickness Compression Modulus (GPa)	D695	7.65	4.96	54
Through-thickness Compression Strength (MPa)	D695	696	455	53
Punch Shear Strength (MPa)	D732	192	128	50
Through-thickness CTE ($\mu\text{m}/(\text{m}^\circ\text{C})$)	E831	28.5	40.8	-30

3.3 Composite Quasi-Static Tensile Behavior

Quasi-static tensile testing of the laminates was done in both the matrix-dominated $\pm 45^\circ$ orientation and the fiber-dominated 0° orientation. Consideration of these two orientations allows separate exploration of the underlying behavior during off-axis and on-axis load cycling. Generally, structures are designed such that primary loads and primary material axes are aligned, but multiaxial loads are carried. Representative stress-strain curves for both orientations are shown in Figure 1.

The high loading of inorganic particles is seen to affect the tensile behavior in both orientations dramatically. (For the $\pm 45^\circ$ orientation the useful part of the deformation response is for strains of a few percent. There is scissoring of the fibers at larger strains. For the control laminate, the test shown was stopped at 10%.) Initial stiffness and peak load are increased. For the 0° orientation, strain at failure is reduced. In the context of the following discussion of fatigue, it is helpful to consider the tensile modulus of the laminate in the $\pm 45^\circ$ orientation rather than using the data to determine the in-plane shear modulus of the laminate.

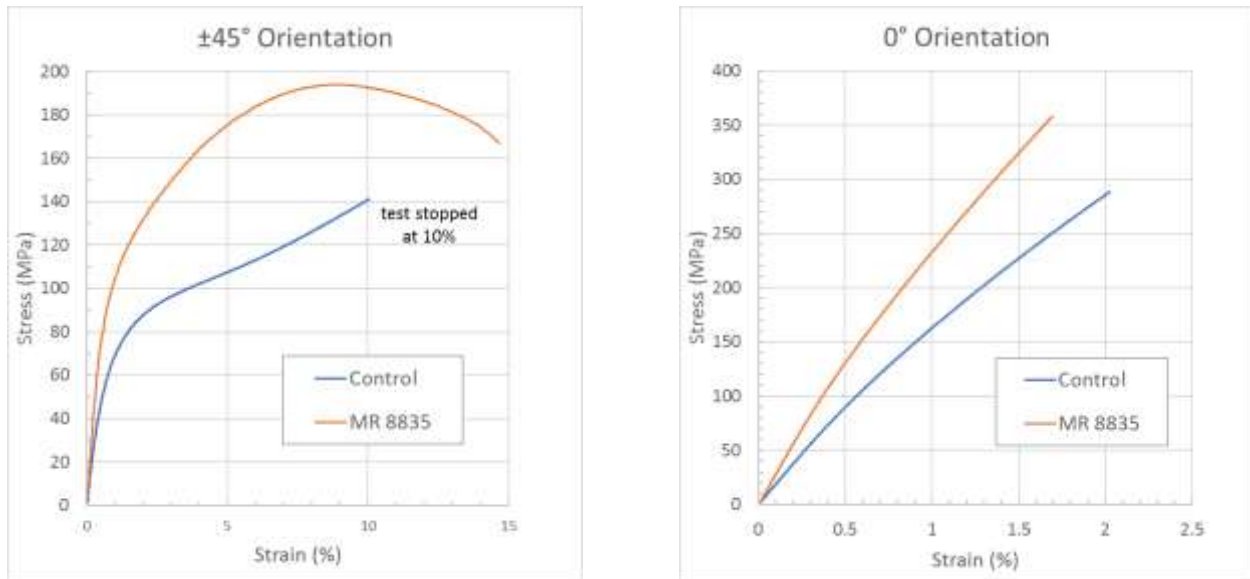


Figure 1. Tensile stress-strain behavior for composite laminates

The average chord modulus taken between 1000 and 3000 microstrain and ultimate properties for the 0° orientation are reported in Table 3 for the 3 specimens tested for each material and orientation.

Table 3. Static Tensile Properties for Laminates

Laminate	±45° Chord Modulus (GPa)	0° Chord Modulus (GPa)	0° Strength (MPa)	0° Failure Strain (%)
Control	11.7	18.5	294	2.08
MR 8835	18.6	26.9	362	1.78

The greater stiffness of the MR 8835 laminate has a direct implication for stress-controlled fatigue. At a given applied stress, the resulting tensile strain is reduced relative to what would be experienced by the control laminate. This is illustrated in Figure 2 for arbitrarily-chosen stresses.

While Figure 2 shows the difference in strain for monotonic loading, during fatigue loading the stress-strain response can change due to accumulation of damage. Such changes were followed during the fatigue testing in this study.

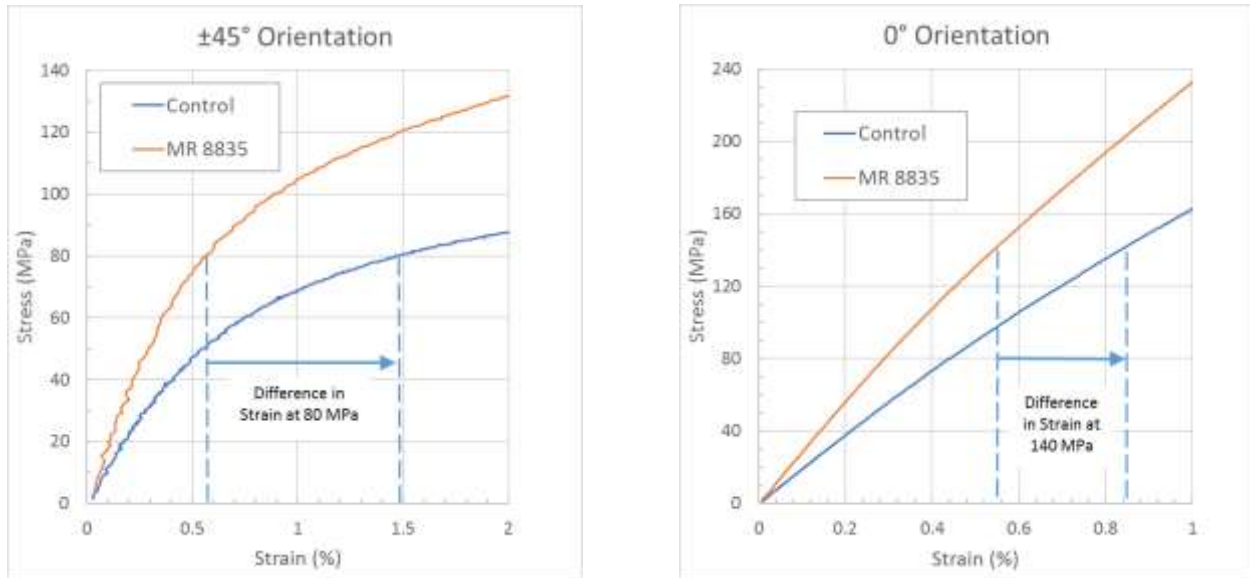


Figure 2. Tensile stress-strain behavior for composite laminates showing the low strain region and strain differences at arbitrary stresses

3.4 Composite Tensile Fatigue Behavior

In the following discussion of fatigue results, the response in the matrix-dominated $\pm 45^\circ$ orientation will be discussed first, then the behavior in the 0° orientation. For each orientation the stress-life curves will be presented, and then the cyclic stress-strain behavior and data for stiffness changes during cycling.

3.4.1 Fatigue Loading in $\pm 45^\circ$ Orientation

Stress levels for fatigue testing were chosen to achieve well-distributed specimen lifetimes of between 10^4 and 10^6 cycles. A few specimens were tested at the same stress levels to suggest repeatability of the results.

3.4.1.1 Stress-Life Curves for $\pm 45^\circ$ Orientation

Stress-life curves for the $\pm 45^\circ$ orientation are shown in Figure 3. Semi-log linear trendline fits through the data represent the behavior well. There are no breaks in the trends over this life range indicating a transition in mechanisms or a fatigue limit. Replicate tests show good reproducibility.

The most notable result of this comparison is the much greater fatigue life of the nanocalcite-modified laminate. For example, at a stress level of 80 MPa, the fatigue life for the control was 14,518 cycles, while the MR 8835 laminate failed at 945,910 cycles—65 times that of the control. For the target range of lifetimes, the imposed stress ranges only overlapped at that one level.

A simple approach to verifying the effect of laminate stiffness illustrated in Figure 2 is to determine the stresses required to achieve the number of cycles to failure and compare the associated strains from the quasi-static stress-strain curves. For example, consider a lifetime of

one million cycles. From Figure 3 the stress for the control is about 55 MPa and for the MR 8835 laminate about 80 MPa. Referring to Figure 2, the strains for these stresses are about the same—slightly over 0.5%. Roughly speaking, the difference in stress required to achieve a given number of cycles to failure for the two materials is due to the difference in stiffness. However, in the next section it will be seen that the quasi-static tensile curves do not generally reflect the true deformation behavior of the materials during accumulation of fatigue damage. Especially for the higher-stress, low-cycle tests, the quasi-static and cyclic behavior can be much different. It should also be noted that the nanocalcite and control matrix resins have critical energy release rate values that are not very different. (See Table 1). For nanoparticle systems formulated for greater toughening, one would expect the difference in accumulated damage to be greater.

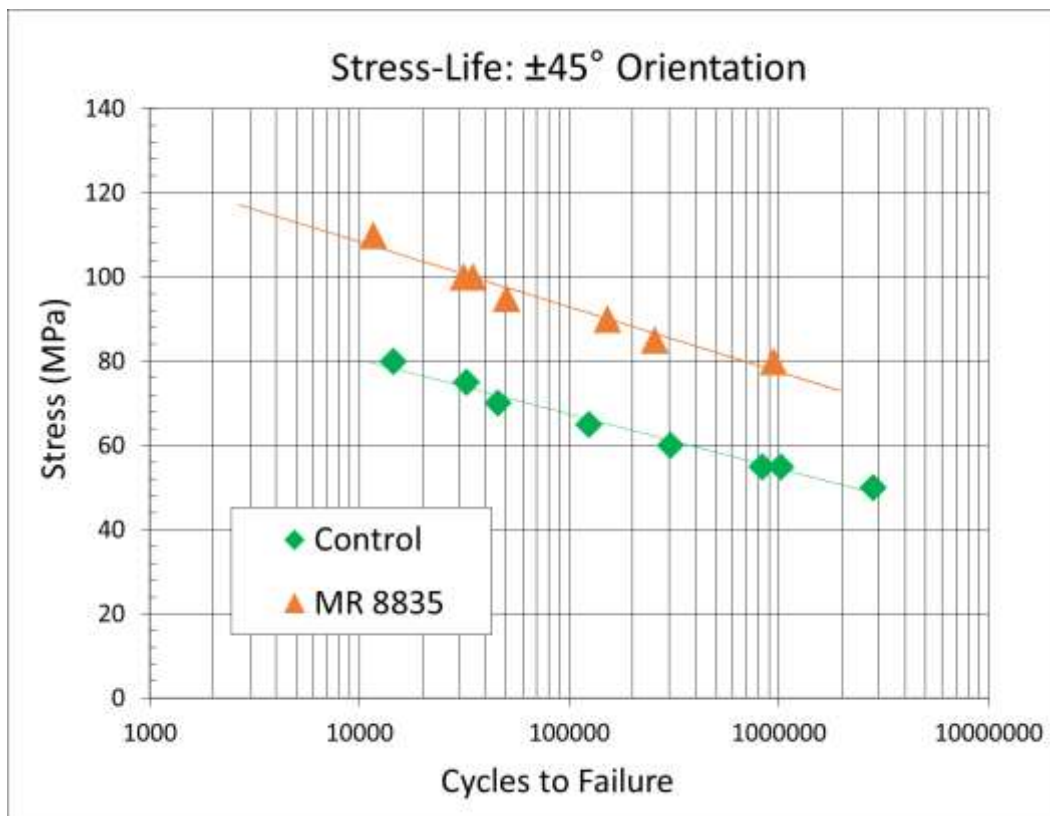


Figure 3. Stress-life curves for laminates in the $\pm 45^\circ$ orientation

3.4.1.2 Stiffness Reduction for $\pm 45^\circ$ Orientation

Load, displacement, and strain were recorded for selected cycles during fatigue testing. Data were captured for cycles 1, 2, 5, 10, 20, 50, 100, etc. until failure. Cyclic stress-strain behaviors for the 80 MPa stress level are shown in figure 4.

The marked difference in the stress-strain loops is solely due to the difference in matrix properties. The control exhibits much more hysteresis as well as ratcheting, the incremental increase in mean strain per loop. First cycle nonlinearity is notable. The MR 8835 laminate shows a modest amount of ratcheting and more closed hysteresis loops. The area enclosed in a

stress-strain hysteresis loop can be interpreted as an energy per unit volume that is dissipated each cycle, either as heat or to drive damage processes such as microcracking.

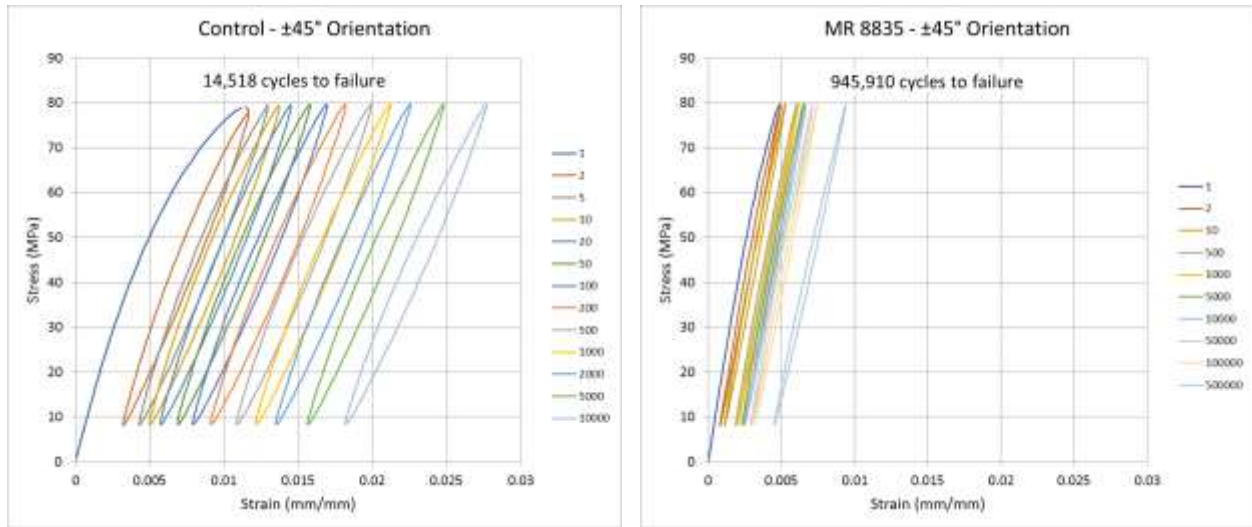


Figure 4. Selected stress-strain loops at the 80 MPa maximum stress level for $\pm 45^\circ$ orientation

In addition to comparing the control and nanocalcite-modified laminate behaviors at a fixed stress level, the behaviors can be compared at similar fatigue life. In Figure 5 the stress-strain loops for a control specimen having a fatigue life of 1,018,402 (55 MPa maximum stress) is compared to loops for the MR 8835 specimen of Figure 4 having a fatigue life of 945,910 cycles (80 MPa maximum stress). The strain scale has been adjusted. In this comparison, the maximum stress for the control is 69% of that for the MR 8835 laminate. Associated with the higher stress for the MR 8835 specimen are greater ratcheting and change in slope than for the control. Equal life was not a simple consequence of similar strain histories.

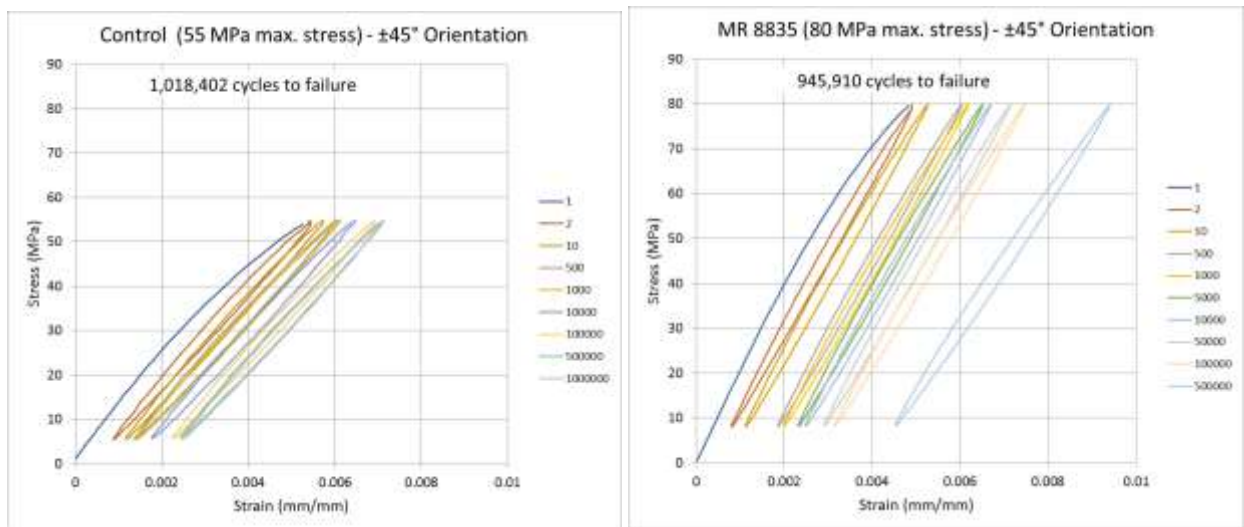


Figure 5. Selected stress-strain loops for nearly equal fatigue life (but different maximum stress) for the $\pm 45^\circ$ orientation

If specimen stiffness is defined as the slope of a line connecting the tips of stress-strain hysteresis loops, the stiffness can be conveniently plotted as a function of loading cycles. Change in stiffness is a helpful indicator of damage in a specimen. Stiffness and mean strain ratcheting together describe the overall cyclic deformation behavior.

During fatigue testing, maximum and minimum values for the load and strain were captured every 100 cycles. Stiffness as a function of loading cycles is plotted in Figure 6. Each curve shows the stiffness for one specimen during cycling. The differing stiffness values at 100 cycles for each material are due to stiffness changes during the first 100 load cycles. In general, specimens displayed a rapid decrease in stiffness at the beginning of the test, followed by an approximately semi-log linear behavior, which is then followed by a turn downward in the stiffness curve that persisted until failure. For lower-stress tests of the control, the third, final stage of stiffness decrease is not seen.

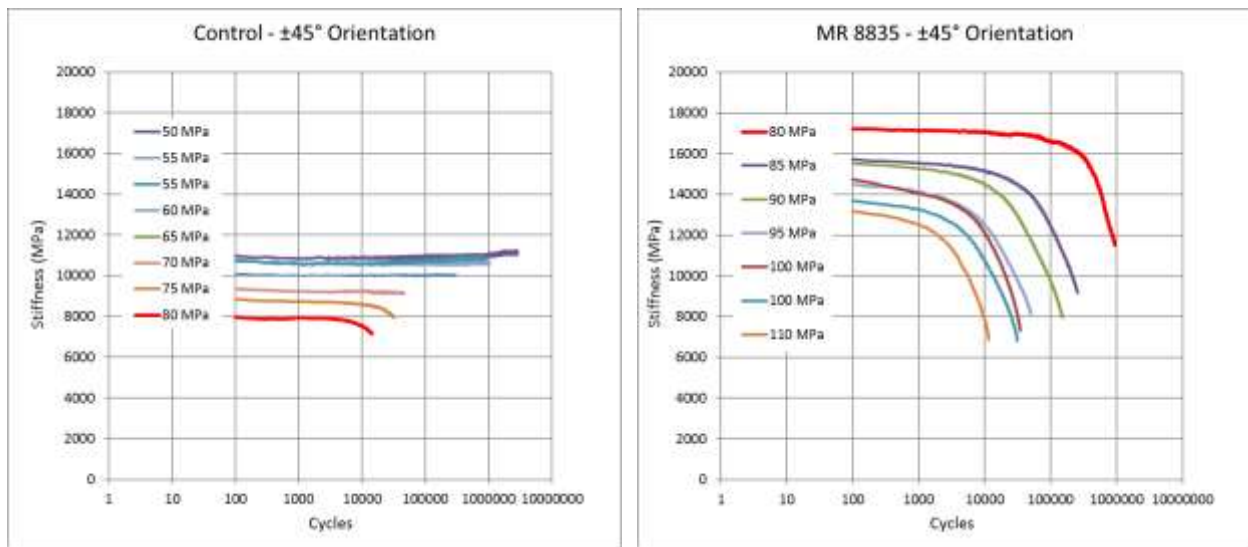


Figure 6. Stiffness as a function of cycles for the $\pm 45^\circ$ orientation laminates

Note that the only overlap in imposed stress for the two data sets shown in Figure 6 is at 80 MPa. (The curves for this stress are red in both plots.) The corresponding cyclic stress-strain loops for these two specimens are shown in Figure 4.

The higher laminate stiffness seen in the quasi-static tensile curves of Figures 1 and 2 is reflected in the much higher stiffness during fatigue cycling after 100 load cycles; the stiffness effect persists after the accumulation of damage during initial cycling. For example, the stiffness of the nanocalcite-modified laminate is over twice the stiffness of the control after 100 cycles at 80 MPa.

It is notable that the change in stiffness is significantly greater for the MR 8835 laminates over the fatigue life range represented here. This can be understood to be a consequence of the role of the matrix in load sharing. Because the stiffer matrix carries a greater portion of the total axial load, the accumulation of damage such as microcracking has a greater effect on the overall stiffness of the laminate during fatigue cycling. However, as noted previously, the stress ranges

for the two data sets are different, so the interpretation of less change in the control (albeit for shorter fatigue life) must take into account very different loading conditions.

3.4.2 Fatigue Loading in 0° Orientation

Stress levels for fatigue testing were chosen to achieve well-distributed specimen lifetimes of between 10^4 and 10^6 cycles. Several specimens were run at the same stress levels to check repeatability of the results.

3.4.2.1 Stress-Life Curves for 0° Orientation

Stress-life curves for the 0° orientation are shown in Figure 7. The semi-log linear trendline fits through the data represent the behavior well. There are no breaks in the trends over this life range indicating a transition in mechanisms or fatigue limit. Replicate tests show good reproducibility.

As was observed for the $\pm 45^\circ$ orientation, the most notable result of this comparison is the much greater fatigue life of the nanocalcite-modified laminate. For the target range of lifetimes, the imposed stress ranges overlapped between 120 and 135 MPa. The increase in life in this range was approximately 10 to 20 times.

Fatigue performance in the 0° orientation is clearly a critical material metric for most fatigue-sensitive designs, since most will align the 0° orientation with the primary loading direction.

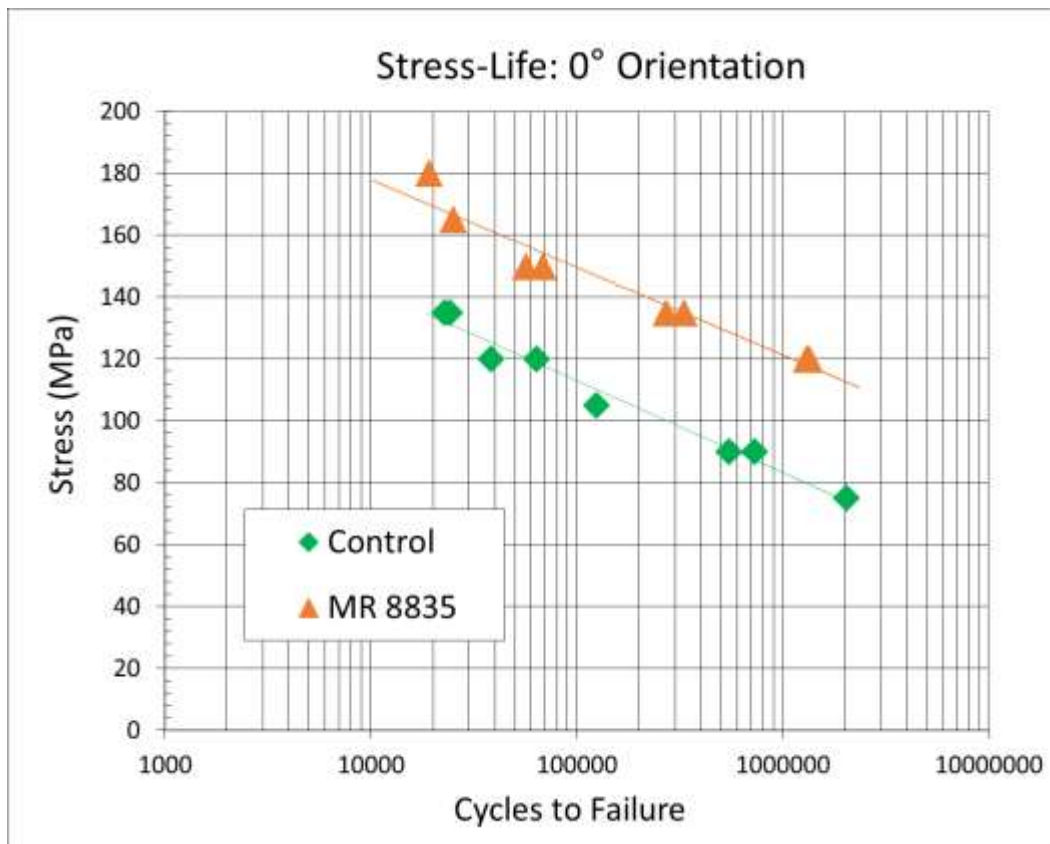


Figure 7. Stress-life curves for laminates in the 0° orientation

3.4.2.2 Stiffness Reduction for 0° Orientation

Stress-strain loops for the 120 MPa stress level are shown in figure 8. Relative to the behavior in the $\pm 45^\circ$ orientation, the amount of hysteresis, stiffness decrease, and strain ratcheting are much less. At this load level, fatigue life is increased approximately 20 times. Increase in mean strain is significantly greater for the control. For the control, the minimum strain of the hysteresis loops is increasing, while for the MR 8835 specimen the minimum strain is constant.

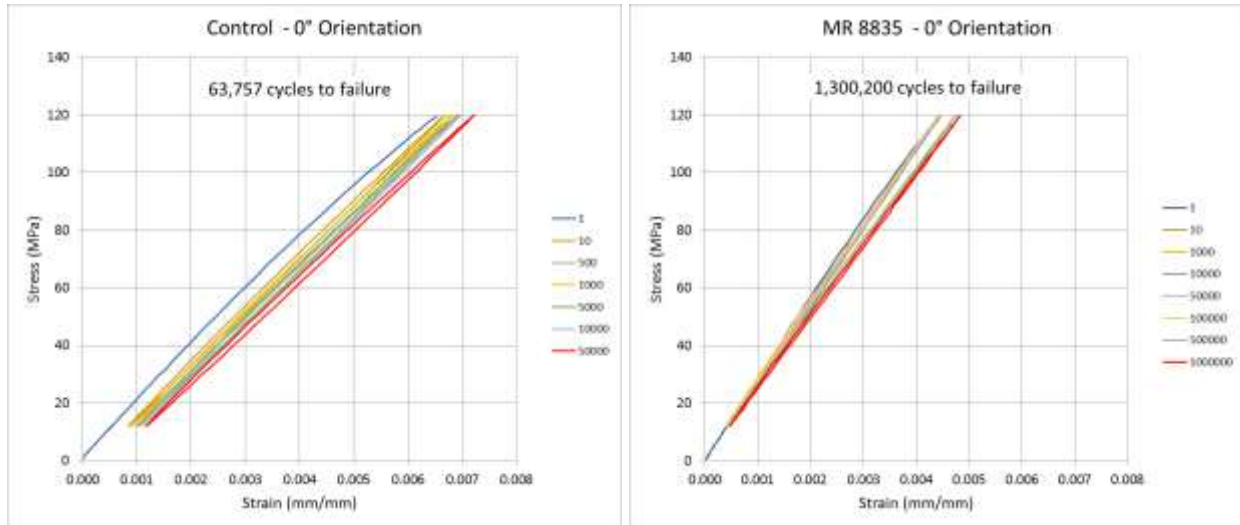


Figure 8. Selected stress-strain loops at the 120 MPa maximum stress level for 0° orientation

For the 0° orientation laminates, most load is transmitted through the glass fibers oriented in the loading direction. Fatigue failure is expected to be dominated by the loading state of those fibers, which is determined by strain in the loading direction. In Figure 9 the stress-strain loops for the control specimen of Figure 8 having a fatigue life of 63,757 (120 MPa maximum stress) is compared to loops for an MR 8835 specimen having a fatigue life of 68,657 cycles (150 MPa maximum stress). In this comparison, the maximum stress for the control is 80% of that for the MR 8835 laminate.

The beginning and ending strain ranges for the control and MR 8835 laminates in Figure 9 are not the same, but are very close, within 0.1% strain. This observation supports the conjecture that the strain range experienced by the fibers in the loading direction controls the fatigue life. This contrasts with the situation for the $\pm 45^\circ$ orientation shown in Figure 5, where the strain ranges are quite different for the control and nanocalcite-modified materials for a similar fatigue life. (It should be noted, also, that the specimen data for Figure 5 is for fatigue lives of about a million cycles, while the Figure 9 comparison is for specimens having much shorter lives.)

The data plotted in Figure 9 for the MR 8835 laminate illustrates that the strain range cannot be accurately predicted based on the quasi-static behavior. For this stress range, damage accumulation during load cycling increases the strain range experienced by the 0° fibers. It is reasonable to hypothesize that for long fatigue lives achieved at lower stress cycling, stress-strain nonlinearity and damage accumulation will be lower, so correspondence with the quasi-static behavior will be better—perhaps enabling correlation of fatigue life through the quasi-static

stress strain curves. This hypothesis will be examined in the light of the data for stiffness as a function of loading cycles.

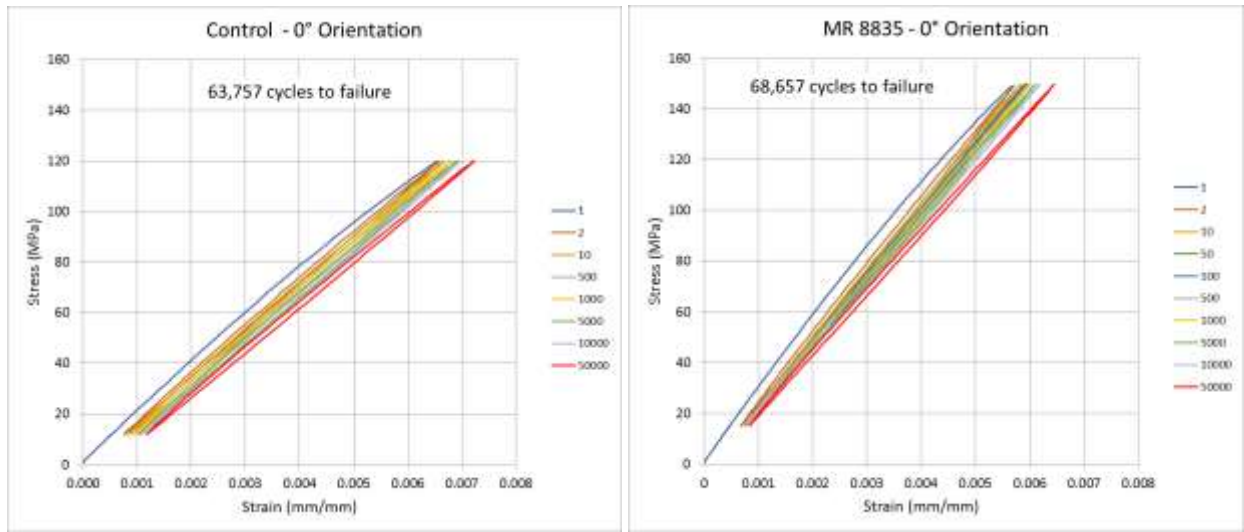


Figure 9. Selected stress-strain loops for nearly equal fatigue life (but different maximum stress) for the 0° orientation

Stiffness as a function of loading cycles is plotted in Figure 10. The stress levels in common for the two data sets are indicated by a red box in the legends.

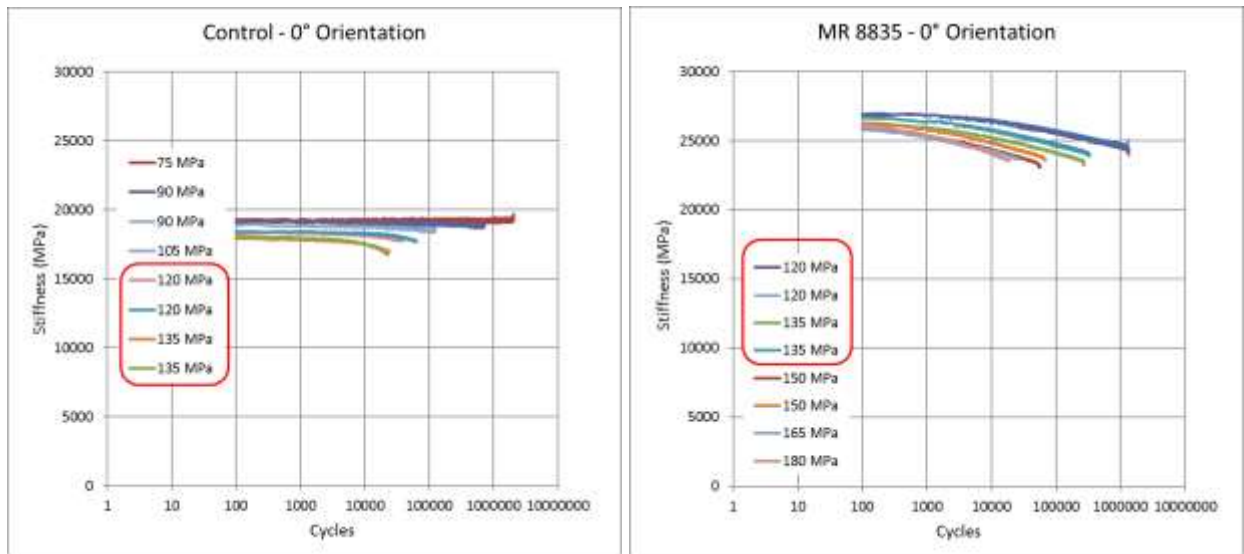


Figure 10. Stiffness as a function of cycles for the 0° orientation laminates

Several differences can be seen when comparing the stiffness as a function of cycles for the 0° orientation laminates in Figure 10 with the behavior for the $\pm 45^\circ$ orientation in Figure 6. The absolute levels of stiffness are much higher, as expected for the 0° fiber-dominated orientation. The range of stiffness at 100 cycles is smaller for each material; initial load cycling has less effect. The relative change in stiffness during cycling to failure is less for the MR 8835 laminate.

As discussed for the $\pm 45^\circ$ orientation results, since the difference in stiffness between the control and nanocalcite-modified material is solely due to the higher stiffness of the matrix, damage accumulation in the matrix will have a larger effect on specimen stiffness for the MR 8835 laminate than for the control. And relative to the $\pm 45^\circ$ orientation, the portion of load sharing by the matrix is less, so change in stiffness is less. Previously the hypothesis was made that for long fatigue lives correlation of fatigue life through the quasi-static stress strain curves might be possible. That would mean that the stresses producing the same fatigue lives for both the control and nanocalcite-based laminates could be predicted by determining the stresses from the stress-strain curves that produce a given strain (e.g., from Figure 2 for the 0° orientation). However, the plot for MR 8835 in Figure 10 shows that there is stiffness change even for the lowest-stress, longest-life tests. The phenomenon of matrix damage accumulation interferes with the strict correlation of the stress-based data using strain, at least for the fatigue life range considered here.

4. SUMMARY AND DISCUSSION

The effect of modifying the matrix of a glass fabric reinforced composite using a high loading of inorganic nanoparticles was studied, focusing on tensile quasi-static and stress-controlled fatigue performance. The matrix-dominated $\pm 45^\circ$ orientation and fiber-dominated 0° laminate orientation were explored.

The primary nanocalcite matrix property that impacted the composite properties was matrix modulus. The high loading of stiff inorganic nanoparticles implemented in MR 8835 translated to increased composite laminate modulus, as would be expected for a multiaxial laminate such as the plain weave fabric that was studied. Previous work had shown that higher matrix modulus could increase composite compression strength. However, the compression strength increase that was measured was of greater magnitude than previously reported. The tensile strength of the laminates was increased, most surprisingly in the 0° laminate orientation, an increase of 20%. The mechanisms for this increase were not explored. Given the significance of the result, understanding of the relative role of simple matrix stiffness and possible micromechanical contributions warrants further study.

A major finding of this study is that the stress-controlled fatigue life of the modified matrix laminate was increased by more than an order of magnitude for the life range studied. This was true for both $\pm 45^\circ$ and 0° laminate orientations.

Cyclic stress-strain behavior showed that for given maximum stress, matrix modification resulted in less hysteresis and strain ratcheting. Throughout cycling to failure, the strain range was significantly lower. Data suggest that the fatigue life for the 0° laminate orientation is associated with the strain range produced by a given maximum stress.

Stiffness in both $\pm 45^\circ$ and 0° laminate orientations was much higher for the nanocalcite-modified laminates than for the control laminate. The higher stiffness was maintained in the 0° laminate orientation throughout cycling to failure for all tests. Changes in stiffness during fatigue cycling were greater for the nanocalcite-modified laminates over the life range tested; as noted, these observations were for specimens having much higher stress levels than for the control.

This study demonstrates that matrix modification with a high loading of stiff inorganic particles can significantly improve the static stress-strain behavior and stress-controlled fatigue performance of a glass fabric reinforced composite. To extend the scope, future work could address strain-controlled fatigue, quasi-isotropic laminates, performance in nonuniform loading (e.g., periodic overload fatigue), and alternative reinforcement forms (e.g., non-crimp fabric, unidirectional prepreg, and carbon fiber).

5. REFERENCES

1. Hackett, S.C., Nelson, J.M., Hine, A.M., Sedgwick, P., Lowe, R.H., Goetz, D.P., Schultz, W.J. "Improved Carbon Fiber Composite Compression Strength and Shear Stiffness through Matrix Modification with Nanosilica." *Proc. American Society for Composites 25th Annual Technical Conference*. Dayton, OH, Sept. 20-22, 2010.
2. Nelson, J., et al. "The Development of Nanosilica-Modified Tooling Prepregs: A Progress Review and New Advances." *CAMX Conference Proceedings*. Orlando, FL. Oct 13-16, 2014. *CAMX – The Composites and Advanced Materials Expo*. CD-ROM.
3. Thunhorst, K., Goetz, D., Hine, A., Sedgwick, P. "The Effect of Nanosilica Matrix Modification on the Improvement of the Pultrusion Process and Mechanical Properties of Pultruded Epoxy Carbon Fiber Composites." *Proc. American Composites Manufacturers Association COMPOSITES 11*. Ft. Lauderdale, FL, Feb. 2-4, 2011.
4. Sharma, A., et al. "Improved Performance of Filament-Wound Composite Drive Shafts with Next Generation Inorganic Nanoparticle-Filled Epoxy Resins." *CAMX Conference Proceedings*. Anaheim, CA, Sept. 26-29, 2016. *CAMX – The Composites and Advanced Materials Expo*.
5. Goenner, E., Thunhorst, K., Goetz, D., Nelson, J. "The Effect of Nanocalcite on the Mechanical Performance of Filament-Wound Composite Overwrapped Pressure Vessels." *CAMX Conference Proceedings*. Anaheim, CA, Dec. 12-14, 2017. *CAMX – The Composites and Advanced Materials Expo*.
6. Manjunatha, C., Taylor, A., Kinloch, A. "The Tensile Fatigue Behaviour of a Silica Nanoparticle-Modified Glass Fibre Reinforced Epoxy Composite." *Composites Science and Technology* 70 (2009): 193-199.
7. Tate, J., et al. "Tension-Tension Fatigue Performance and Stiffness Degradation of Nanosilica-Modified Glass Fiber-Reinforced Composites." *Journal of Composite Materials* 52 (2017): 823-834.
8. Makeev, A., et al. "Advanced Composite Materials Technology for Rotorcraft through the Use of Nanoadditives." *Journal of the American Helicopter Society* 60 (2015): 1-10.
9. ASTM Standard Specification D4029/D4029M – 16 "Standard Specification for Finished Woven Glass Fabrics" ASTM International, West Conshohocken, PA, 2016, www.astm.org.
10. Uddin, M.F., Sun, C.T. "Strength of Unidirectional Glass/Epoxy Composite with Silica Nanoparticle-Enhanced Matrix." *Composites Science and Technology* 68 (2008):1637-1643.